Supplementary information

Stability and performance improvement of cesium tin halide perovskites with Astaxanthin treatment.

Barbara Nakamanya[1], Nan Yu[1], Tonny Kakooza[1] Qianwen Sun[1], Andrew Balilonda[2], Shengyuan Yang[*1], and Meifang Zhu[1]

[1]State Key Laboratory for Modification of Chemical Fibers and Polymer Materials, International Joint Laboratory of Advanced Fibers and Low-dimension Materials, College of Materials Science and Engineering, Donghua University, Shanghai 201620, People's Republic of China.

[2]Research Centre for Smart Wearable Technology, School of Fashion and Textiles, The Hong Kong Polytechnic University, Hung Hom, Kowloon, Hong Kong 999077, P. R. China.

Correspondence: cmseysy@dhu.edu.cn (Shengyuan Yang)

Experimental section

Materials:

Cesium Iodide (CsI, 99.9%), Tin iodide (SnI_2, 99.9%), Tin fluoride (SnF_2, 99.9%) were purchased from Shanghai Aladdin Biochemical Technology, Astaxanthin (C40H52O4, 96%) was purchased from Macklin. N, N-Dimethylformamide (DMF, anhydrous 99.8%) and Dimethyl sulfoxide (DMSO, anhydrous 99.8%) were purchased from sigma. Copper Iodide (CuI, 99.95%) was purchased from Shanghai Aladdin Biochemical Technology, Phenyl-C61-butyric acid methyl ester (PCBM, 99.5%) was purchased from Sigma, Zinc Oxide (ZnO, 99.9%) was purchased from Meryer, Silver (Ag, 99%) was purchased from Sigma. All the chemicals were used without further purification.

Solution preparation:

CuI solution was prepared by dissolving 15mg CuI in 1ml of Acetonitrile and ultra-sonicated at room temperature for 1 h. The 0.8M $CsSnI_3$ perovskite solution was prepared by adding CsI, SnI_2 and SnF_2 in a molar ratio of 1:1:0.1 into 1ml of DMF: DMSO solution (8:2, volume ratio) and stirred for a couple of hours to completely dissolve the precursors. Different volume concentrations (0%, 0.2%, 0.5% and 0.8%) of 0.02M AXT solution were added to perovskite solutions and stirred for 1 h. 20mg of PCBM were dissolved in 1ml of chlorobenzene and stirred for 3 h at 60 ^{0}C. 1.4 mg of ZnO was dissolved in 1ml of ethanol and stirred for 1 h and finally all solutions were filtered.

Device fabrication:

The ITO glasses were thoroughly cleaned through ultra-sonicating them in detergent solution, acetone, isopropanol, deionized water for 15 min respectively. The glasses were then blow dried using nitrogen and later O_2 –plasma treated for 5min before use. The fabrication was carried out in a N_2-filled glove box. CuI solution was spin-coated onto the ITO substrates at 3000 rpm for 40 s and annealed at 100 ^{0}C for 10 min. The perovskite solution was later spin-coated on top of the CuI/ITO layer at 1000 rpm for 15 s and 5000 rpm for 40 s. The films were later annealed at 80 ^{0}C for 10 min. The PCBM solution was spin coated at 1000 rpm for 50 s and 5000 rpm for 10 s later annealed at 100 ^{0}C for 10 min. The ZnO solution was also spin coated at 3000 rpm for 30 s and dried for 60 s. Finally, ~ 80nm Ag electrode was evaporated on top of the film.

Characterization:

The XRD patterns were measured using a Shimadzu XRD 6000 diffractometer with Ni filtered Cu Kα radiation. SEM characterizations were conducted on a Field emission scanning electron microscope. Fourier transform infrared microscope and spectrometer (FTIR, a Nicolet TM 6700, 4000 - 400 cm^{-1} range system) in attenuated total reflection (ATR) mode. The absorption spectra were scanned using a Perkin Elmer UV-Vis spectrometer. Steady state and Time resolved photoluminescence was measured using Edinburgh, UK FLS-1000 Steady State Transient Fluorescence Spectrometer with an excitation wavelength of 800 nm. EIS measurements were conducted on Zahner electrochemical workstation. The EQE was performed on a standard test system equipped with a xenon lamp, a Si detector, a monochromator and a dual channel power meter. The J-V curves for 0.5 cm^2 area devices were obtained using a Keithley 6517 source meter under 100 mW/cm^2 AM 1.5G simulated irradiation from a solar simulator.

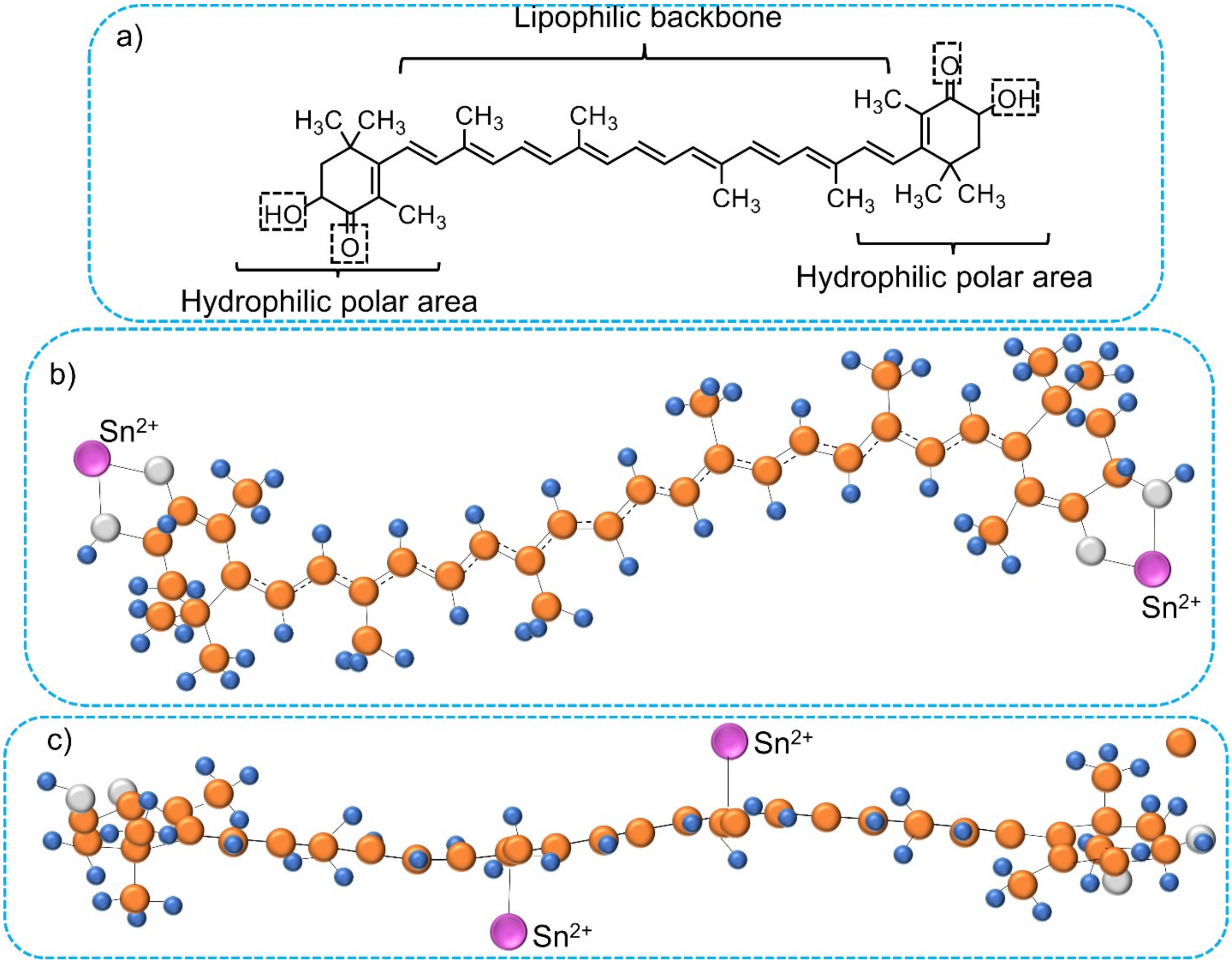

Supplementary figure 1. a) Schematic diagram of the chemical structure of Astaxanthin, b) and c) illustration of the interaction between AXT and the Sn^{2+} from CsSnI$_3$.

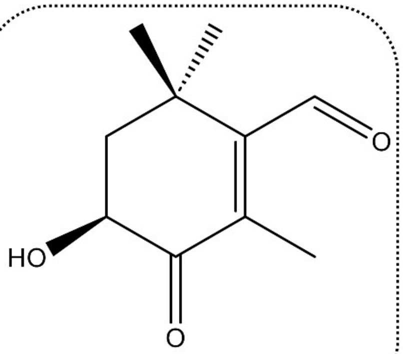

7- Apoastaxanthinal

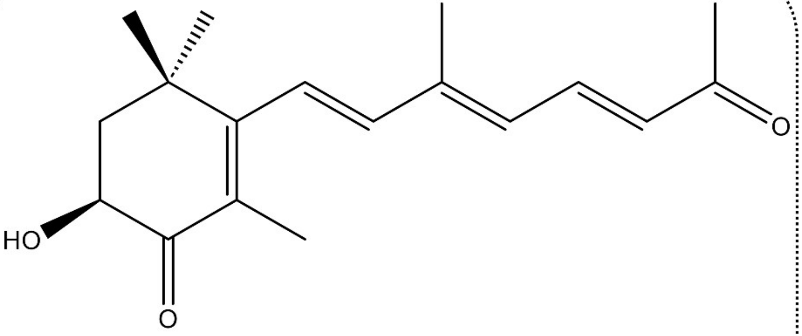

13 - Apoastaxanthinone

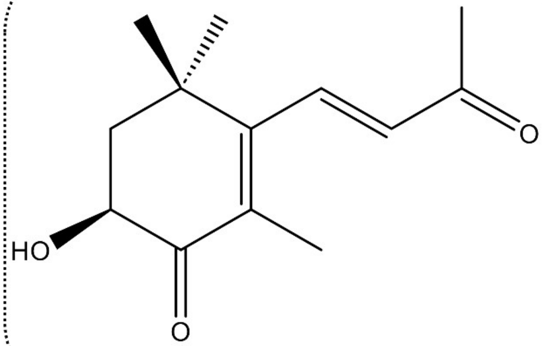

9 - Apoastaxanthinone

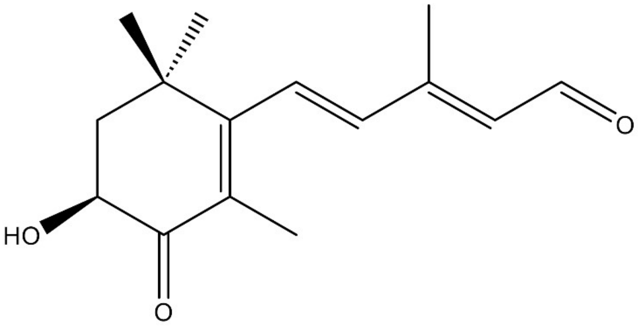

11- Apoastaxanthinal

Supplementary figure 2. Chemical structures of different Apoastaxanthinones and Apoastaxanthinals.

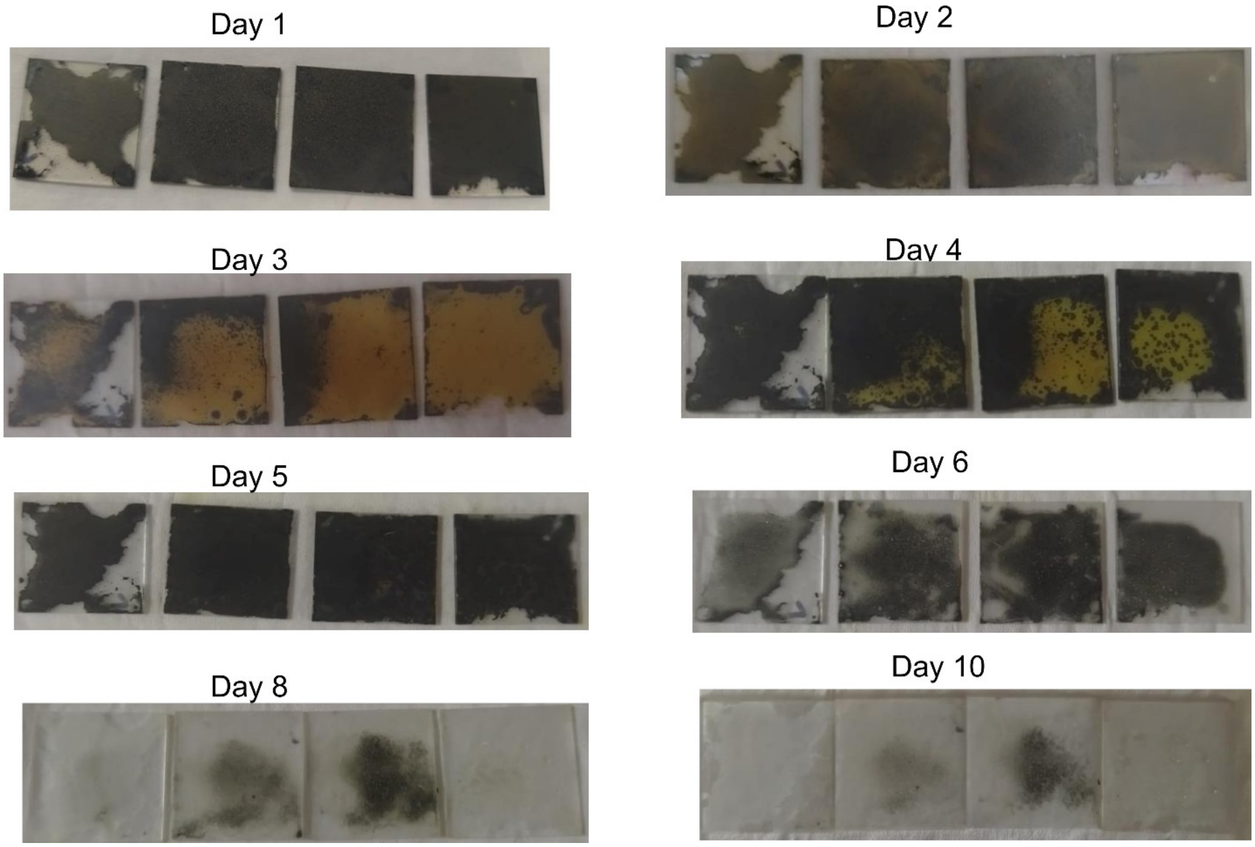

Supplementary figure 3. The degradation and re-construction of our perovskite films. The images of films from the left to right represent 0%, 0.2%, 0.5% and 0.8% of AXT.

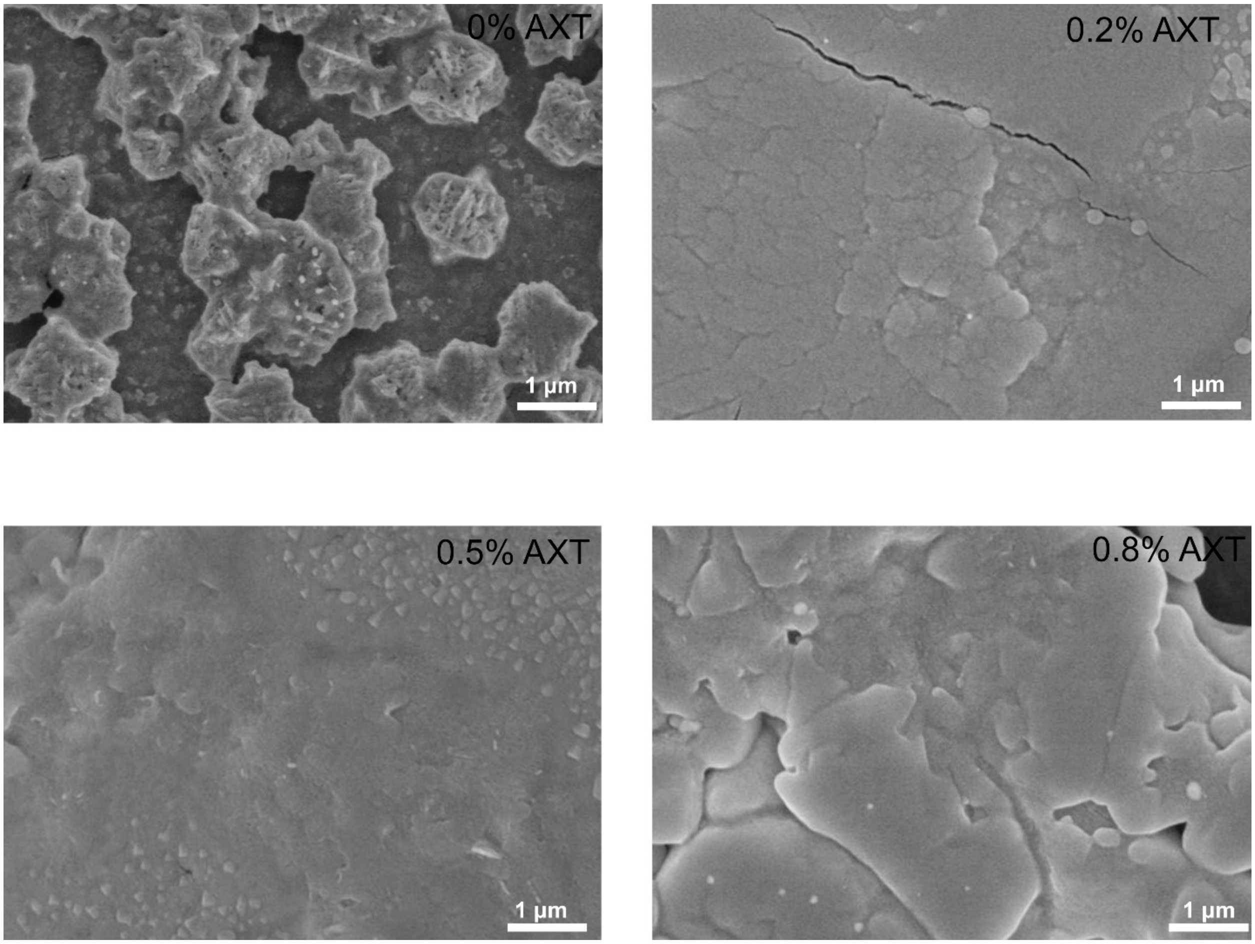

Supplementary figure 4. SEM images for B-samples.

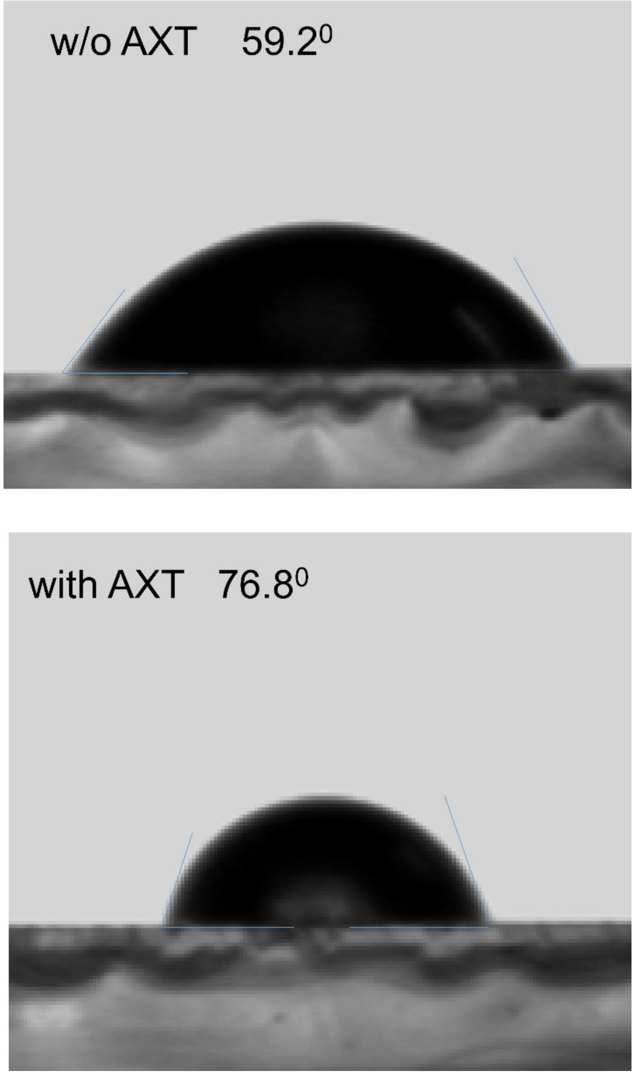

Supplementary figure 5. Water contact angles for with and w/o AXT perovskite films.

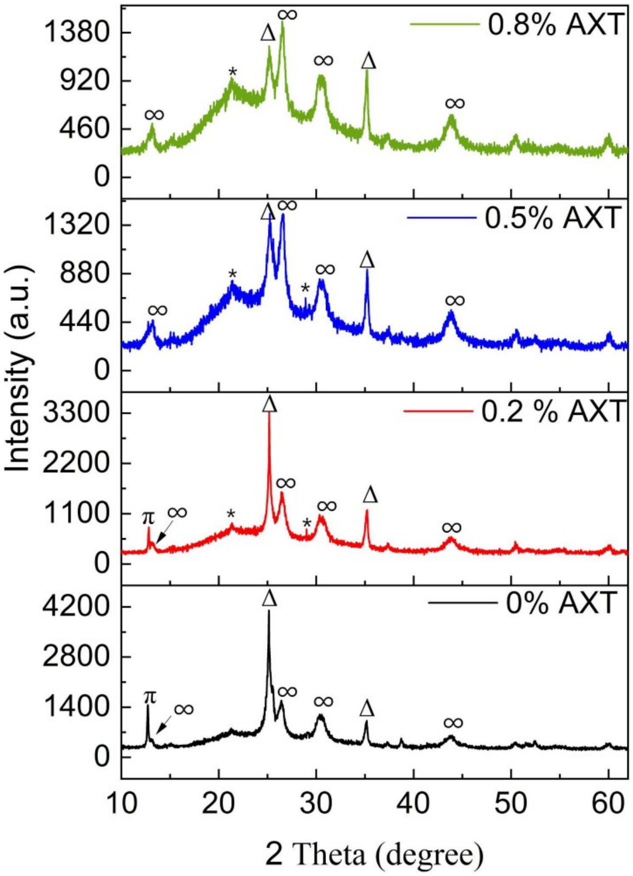

Supplementary figure 6. XRD patterns for B-samples ('∞' symbol represents the Cs_2SnI_6, 'Δ' symbol represents the Y-$CsSnI_3$, '∗' symbol represents γ-$CsSnI_3$, 'π' symbol represents SnI_2).

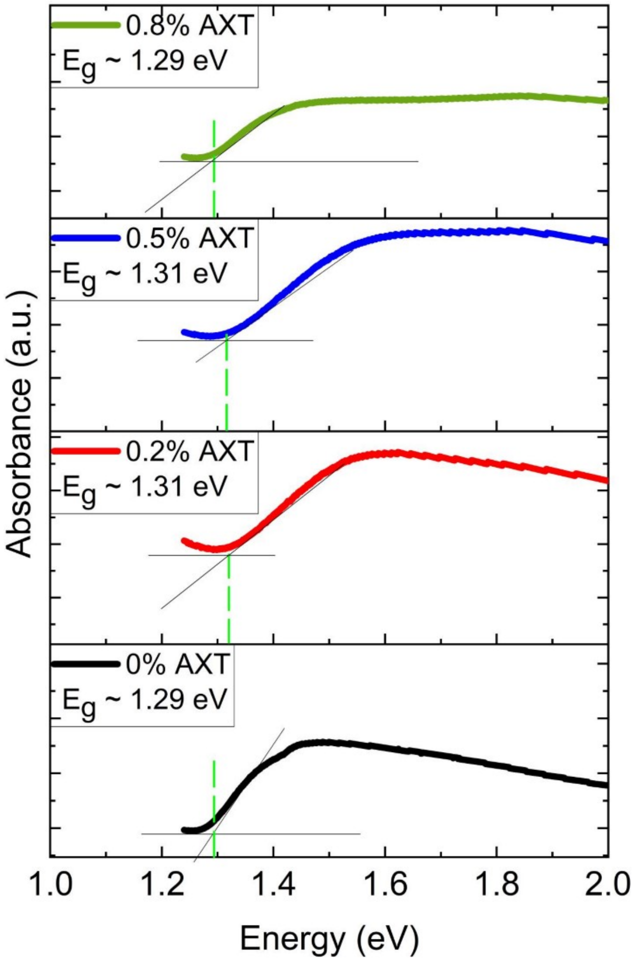

Supplementary figure 7. Tauc plots for determining bandgap.

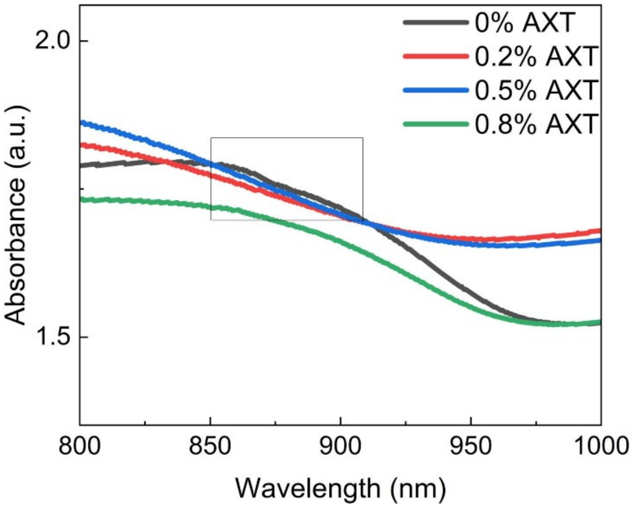

Supplementary figure 8. Increase in absorption for A1 sample.

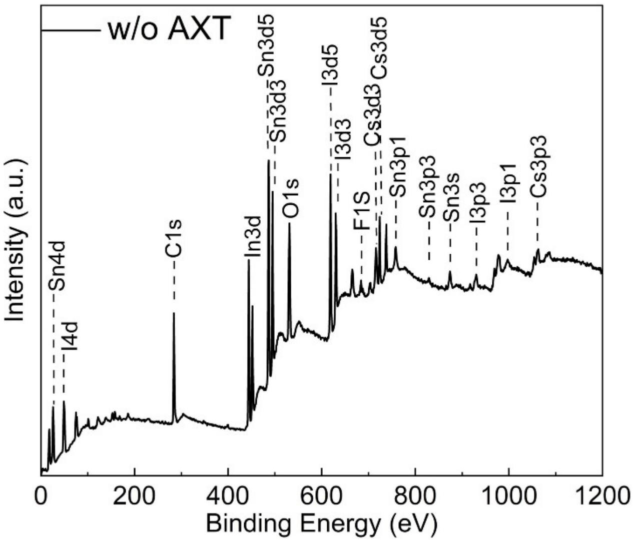

Supplementary figure 9. Wide XPS scan for $CsSnI_3$ w/o AXT.

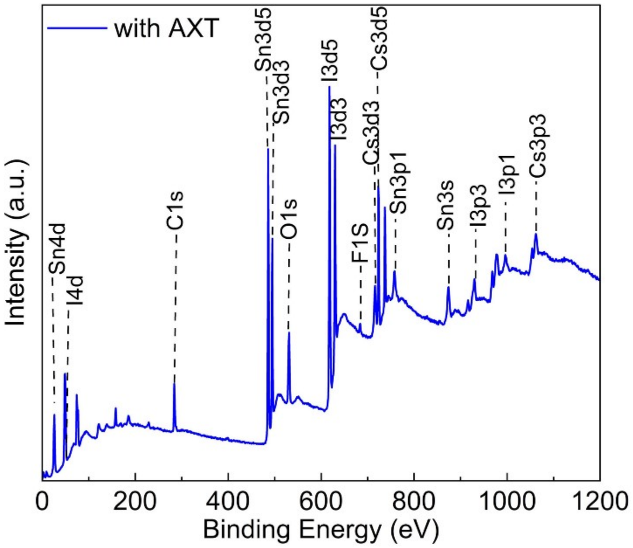

Supplementary figure 10. Wide XPS for $CsSnI_3$ with AXT.

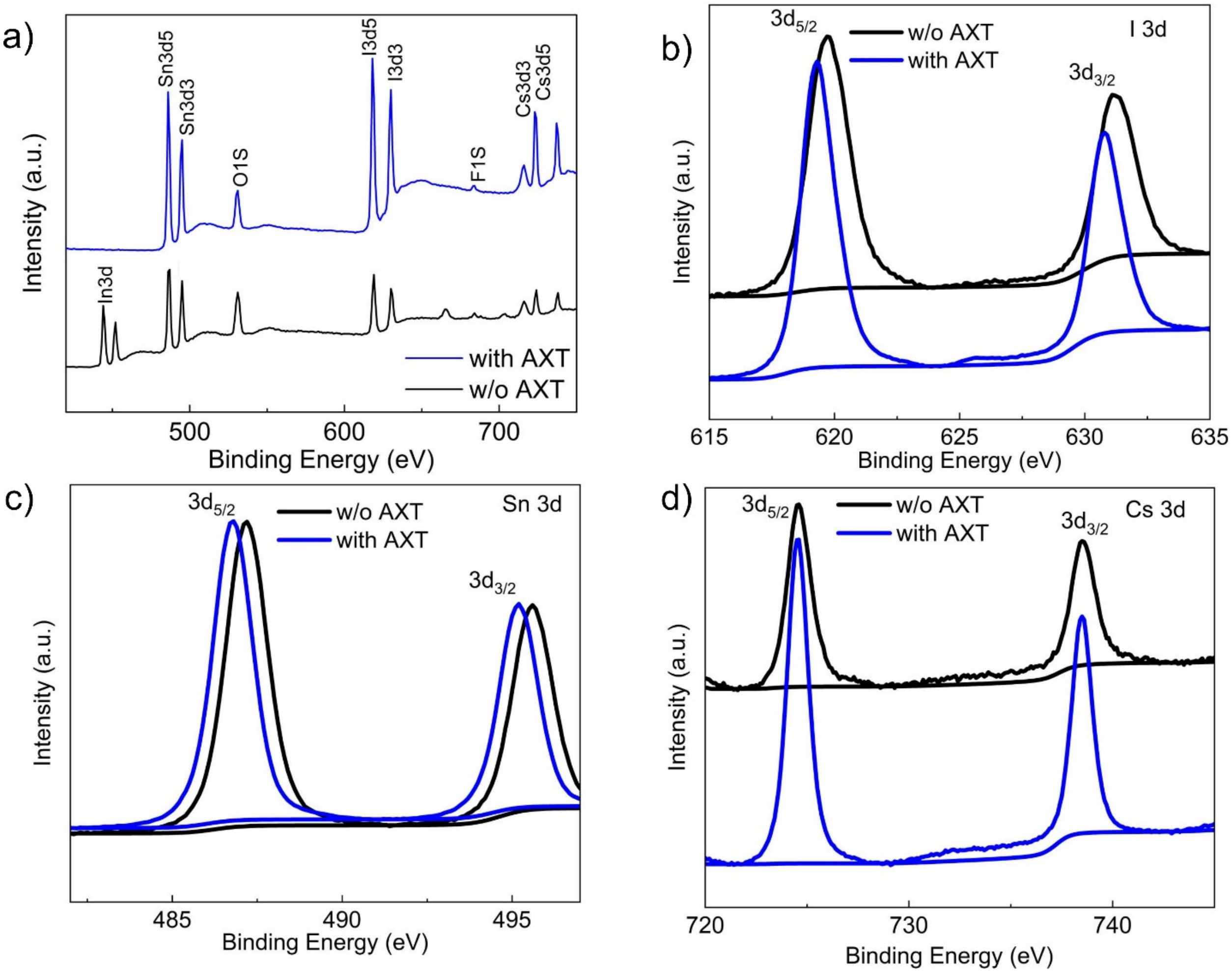

Supplementary figure 11. a) XPS spectrum showing a shift in the peaks to lower binding energies, b - d) individual fitting peaks for Cs3d, Sn3d and I3d.

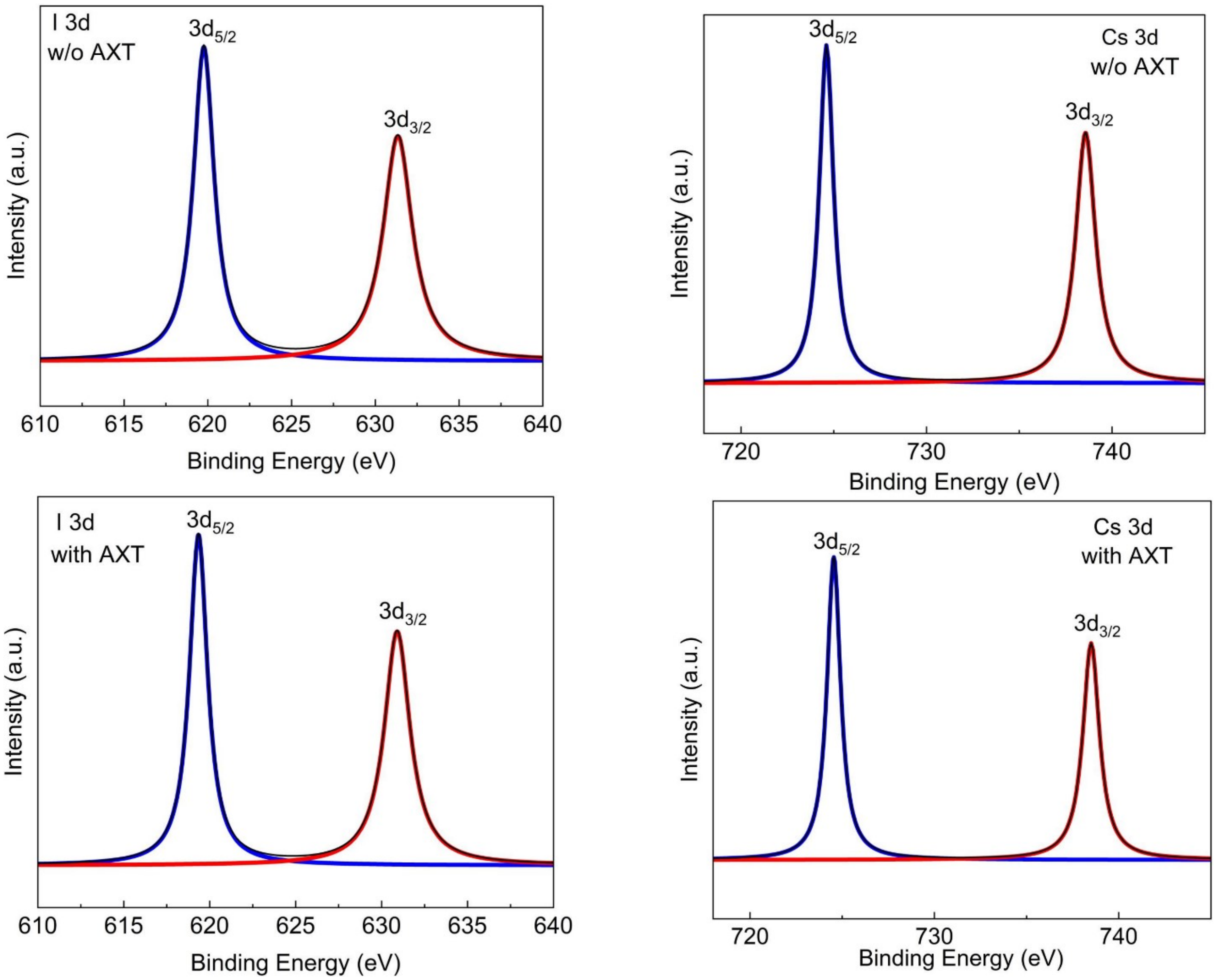

Supplementary figure 12. Individual peak fitting for I3d and Cs3d for w/o AXT and with AXT samples.

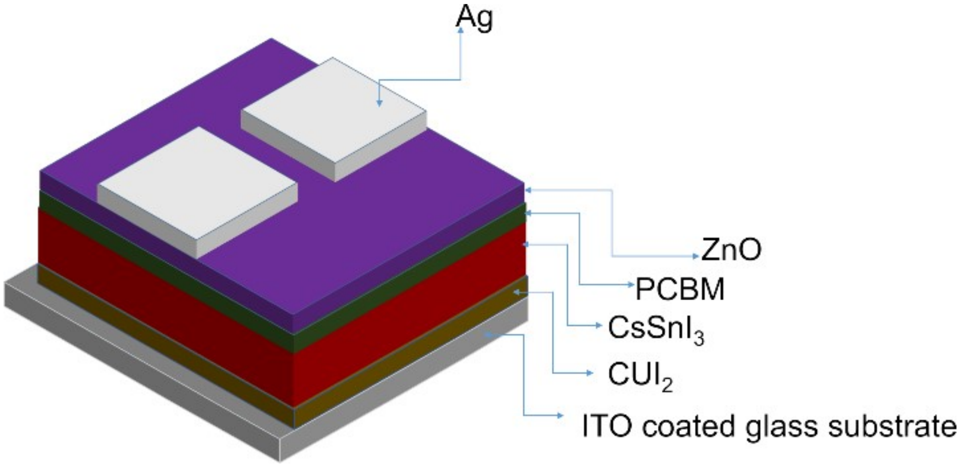

Supplementary figure 13. schematic illustration of our solar cell structure.

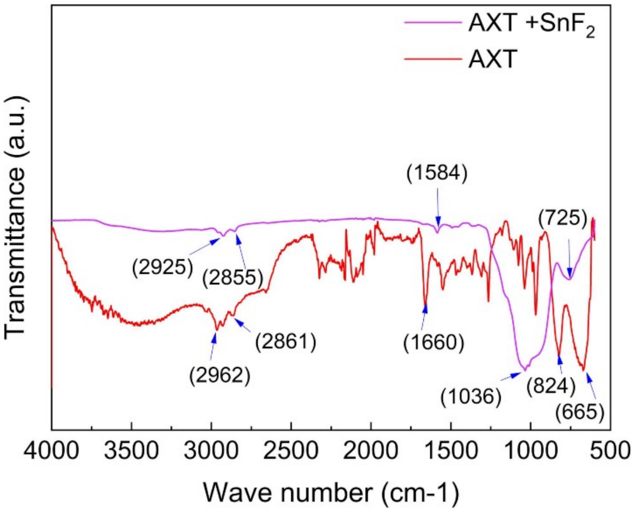

Supplementary figure 14. FTIR showing the coordination interaction between pure AXT and SnF_2.

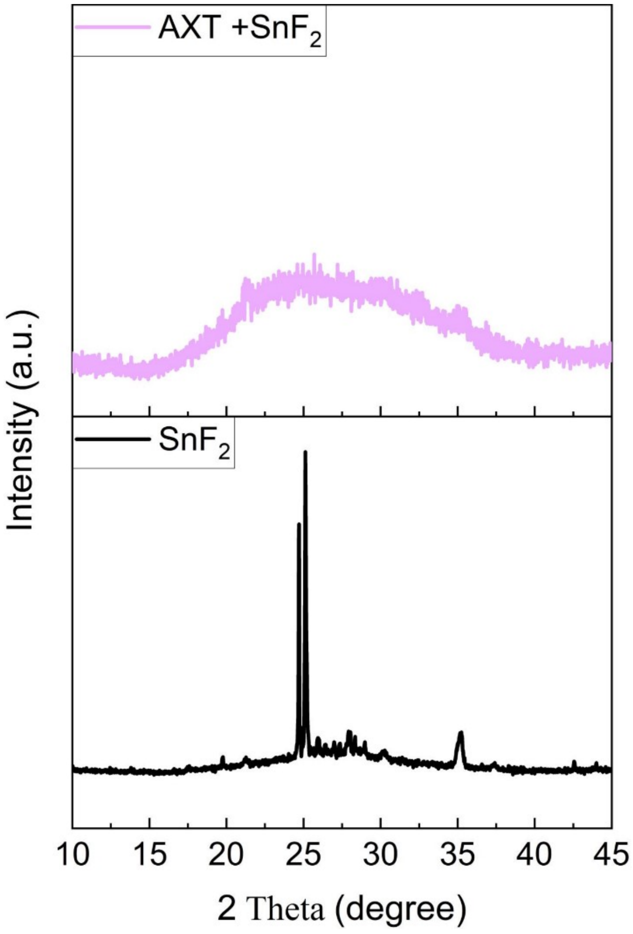

Supplementary figure 15. XRD for pure SnF_2 and the amorphous layer formed due to AXT-SnF_2 complex.

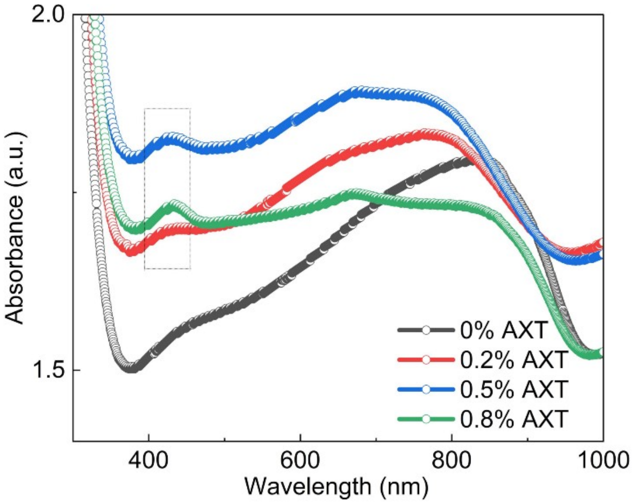

Supplementary figure 16. Dotted area indicating the minor peaks that symbolize absorbance enhancement due to AXT treatment.

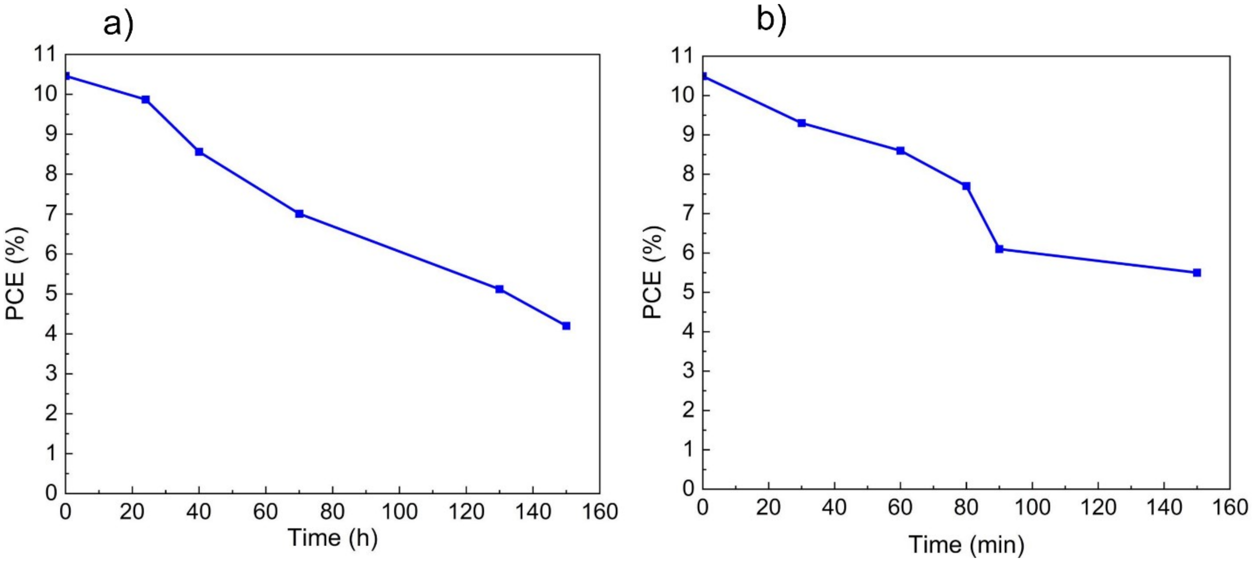

Supplementary figure 17. a) PCE evolution for un-encapsulated device treated with AXT and stored in ambient conditions (RH~60%, RT), b) light soaking stability of the AXT treated device.

Sample	A_1	τ_1 (ns)	A_2	τ_2 (ns)
$CsSnI_3$	13.077	1.119	0.457	6.720
$CsSnI_3$+0.5% AXT	1.219	3.981	0.562	13.019

Supplementary Table 1. Summary of fitted parameters from the TRPL spectra which were fitted using a double exponential equation.

Sample w/o AXT	Cs3d$_{5/2}$	Cs3d$_{3/2}$	Sn3d$_{5/2}$	Sn3d$_{3/2}$	I3d$_{5/2}$	I3d$_{3/2}$
P.position	724.60	738.57	487.19	495.62	619.76	631.34
FWHM	0.92	1.30	1.28	1.48	1.50	2.12
R.Intensity	56516.64	41869.43	219466.62	155610.02	117763.83	84335.02

Supplementary Table 2. Summary of individual peak fitting parameters for C3d, Sn3d and I3d for the sample w/o AXT. (P. position, FWHM and R. Intensity symbolized peak position, full width half maximum and relative intensity respectively).

Sample with AXT	Cs3d$_{5/2}$	Cs3d$_{3/2}$	Sn3d$_{5/2}$	Sn3d$_{3/2}$	I3d$_{5/2}$	I3d$_{3/2}$
P.position	724.54	738.50	486.78	495.21	619.34	630.90
FWHM	0.88	1.08	1.21	1.38	1.27	1.81
R.Intensity	217469.02	155668.01	352920.35	249928.38	382206.98	270428.05

Supplementary Table 3. Summary of individual peak fitting parameters for C3d, Sn3d and I3d for the sample with AXT. (P. position, FWHM and R. Intensity symbolized peak position, full width half maximum and relative intensity respectively).

AXT %	V_{OC} (V)	J_{SC} (mA/cm^2)	FF (%)	PCE (%)
0	0.46	14.28	65.08	4.27
0.2%	0.56	24.06	66.48	8.95
0.5%	0.59	26.05	68.33	10.5
0.8%	0.49	19.75	65.80	6.38

Supplementary Table 4. Photovoltaic parameters for $CsSnI_3$ based PSCs with and w/o AXT.

AXT %		V_{OC} (V)	J_{SC} (mA/cm^2)	FF (%)	PCE (%)
0	RS	0.46	14.28	65.08	4.27
	FS	0.39	14.16	61.49	3.39
0.5%	RS	0.59	26.05	68.33	10.5
	FS	0.58	25.84	65.54	9.82

Supplementary Table 5. Photovoltaic parameters for forward and reverse scans for $CsSnI_3$ based PSCs with and w/o AXT.